Modeling of Natural Organic Matter Transport Processes in Groundwater

T-C. Jim Yeh,[1] Josep Mas-Pla,[2] John F. McCarthy,[3] and Thomas M. Williams[4]

[1]Department of Hydrology and Water Resources, The University of Arizona, Tucson, Arizona; [2]Unitat de Geodinamica Externa i Hidrogeologia, Departamento de Geologia, Universitat Autonoma de Barcelona, Bellaterra, Spain; [3]Environmental Sciences Division, Oak Ridge National Laboratory, Oak Ridge, Tennessee; [4]Baruch Forest Science Institute, Clemson University, Georgetown, South Carolina

A forced-gradient tracer test was conducted at the Georgetown site to study the transport of natural organic matter (NOM) in groundwater. In particular, the goal of this experiment was to investigate the interactions between NOM and the aquifer matrix. A detailed three-dimensional characterization of the hydrologic conductivity heterogeneity of the site was obtained using slug tests. The transport of a conservative tracer (chloride) was successfully reproduced using these conductivity data. Despite the good simulation of the flow field, NOM breakthrough curves could not be reproduced using a two-site sorption model with spatially constant parameters. Preliminary results suggest that different mechanisms for the adsorption/desorption processes, as well as their spatial variability, may significantly affect the transport and fate of NOM. — Environ Health Perspect 103(Suppl 1):41–46 (1995)

Key words: natural organic matter, sorption processes, tracer test, hydrologic heterogeneity, spatial variability, groundwater pollution

Introduction

Hydrologic and chemical factors governing the transport of natural organic matter (NOM) and colloidal particles in groundwater are topics of increasing interest because of their roles in groundwater pollution problems and bioremediation techniques. In particular, NOM has been observed to facilitate the transport of contaminants, otherwise immobile (*1*). Although the sorption mechanisms of NOM to mineral phases have been examined at a laboratory scale (*2*), little is known about the transport processes at a field scale.

In this article, we present some preliminary results of a forced gradient tracer experiment designed to investigate the transport of NOM in a sandy aquifer. Our goal is to characterize the hydrologic properties of the site and their spatial variability so that the chemical interactions governing the NOM migration could be clearly identified. To achieve this goal, slug tests were conducted to depict the detailed three-dimensional hydraulic conductivity distribution of the experimental field site. A three-dimensional flow and solute transport model along with the hydraulic conductivity data were then used to reproduce the movement of a conservative tracer (chloride) injected into the aquifer, as a means to evaluate the accuracy of the numerical model. Once the numerical model was verified, we studied the chemical processes by comparing the observed NOM movement with that simulated by the model with parameters derived from laboratory experiments and previous field tests (*3*).

This paper was presented at the Joint United States–Mexico Conference on Fate, Transport, and Interactions of Metals held 14–16 April 1993 in Tucson, Arizona.

This research is supported by the Subsurface Science Program, Environmental Sciences Division, US Department of Energy, under contract DE-AC05-84OR21400 with Martin Marietta Energy Systems, Inc., and grant DE-FG02-91ER61199.

Address correspondence to Dr. T-C. Jim Yeh, Department of Hydrology and Water Resources, The University of Arizona, Tucson, Arizona 85721. Telephone (602) 621-5943. Fax (602) 621-1422.

Materials and Methods

Field Site Characteristics

The experimental field site is situated at the Hobcaw Field in the Baruch Forest Science Institute, Georgetown, South Carolina. The unconfined shallow aquifer underlying the test site consists of a sandy coastal material, approximately 3 m thick, bounded by an impervious clay layer at the bottom. The test bores gave a general description of the aquifer material which showed a layered structure with coarser sand at the bottom. The clay content of the aquifer material was low, ranging from 9% at the top to 2% at the bottom of the aquifer. Solid phase organic matter content in the aquifer was constant at approximately 0.03%. The water table was approximately 1 m below the ground surface. The average measured hydraulic gradient using daily data from four piezometer surrounding the test site was estimated to be 0.0224, with an orientation of N59°W.

A small 5 x 5 m^2 area was selected for the study of NOM transport using the two-well tracer test method. Injection and withdrawal wells were located 5 m apart (Figure 1). These wells consisted of PVC pipes, 5 cm in diameter, screened from 1 m below the ground surface to the bottom of the aquifer. They were capped at the bottom and equipped with a seal at the top to aid forced injections. A total of 32 observation wells were drilled between the injection and withdrawal wells (Figure 1). Each observation well is constructed with a 2.54 cm diameter pipe, screened from 1 m below the surface to the bottom of the aquifer. Before the tracer experiment, slug tests using packers were performed at 11 depths in each well to determine the three-dimensional hydraulic conductivity distribution of the site. In each well the tests were conducted at an interval of 15.2 cm. There were a total of 248 conductivity measurements after discarding some unreliable tests. After the slug tests, point sampling ports were installed along each well at 1.4, 1.7, 2.0, 2.3, and 2.6 m below the surface to collect the tracer data.

Two-well Tracer Test Methodology

The two-well tracer test consisted of simultaneous injection and withdrawal of water

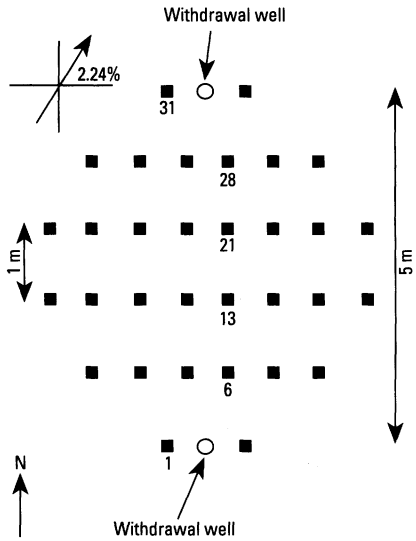

Figure 1. Well distribution pattern at the Georgetown site. Squares represent the observation wells.

at equal rates at the injection and withdrawal wells, respectively, to create a steady-state forced gradient flow field. After the flow reached steady-state, the injected water was supplemented by the tracer concentrations. Flow rates and tracer input concentrations were controlled and calibrated on a daily basis and the injected concentration was periodically recorded. Once the tracer injection ended, input concentrations were kept at the groundwater background levels. During the test the withdrawn water was discharged into a distant stream, down-gradient from the site.

Two forced gradient experiments were performed at the Georgetown site, and their characteristics are presented in Table 1. The first test (May 1992) consisted of a short injection of chloride only (KCl), and it was conducted with the aim to check our capability of modeling the flow field created by the well dipole using the hydraulic conductivity data obtained from slug tests. Once the model was verified it was used to design the sampling scheme for the next test conducted August–September 1992, which involved the simultaneous injection of chloride and NOM. The goal of this test was to study the chemical processes controlling the migration of NOM using chloride as a reference.

Table 1. Characteristics of the two-well tracer tests.

	Test 1 May 1992	Test 2 Aug–Sep 1992
Injection rate	3.8 l min^{-1}	3.0 l min^{-1}
Withdrawal rate	3.8 l min^{-1}	4.5 l min^{-1}
Chloride		
Injected mean C	240 mg l^{-1}	72 mg l^{-1}
Pulse duration	16 hours	662 hr
Background C	11 mg l^{-1}	13 mg l^{-1}
NOM		
Injected mean C	—	32 mg l^{-1}
Pulse duration	—	662 hr
Background C	—	2 mg l^{-1}

Chloride was selected as a suitable tracer because of its conservative behavior, especially in sandy soils, and because the low chloride background of the aquifer (approximately 12 mg l^{-1}). NOM was obtained from a wetland pond near the site which drains from a mixed hardwood forest and the "brown water" contains high levels of NOM. Before injection NOM solution (0.2 μm) was filtered and its oxygen content removed to maintain the anoxic conditions of the aquifer. Tracers were injected as step inputs; however, chloride injection during the second test was highly variable due to mechanical problems.

Sampling Strategy and Analytical Techniques

During the first test, samples were collected at all the sampling ports to obtain a three-dimensional distribution of the chloride plume. Samples were taken from all depths at five wells simultaneously at a rate of 100 ml min^{-1}, starting from locations closer to the injection well. "Snapshots" were taken every 2 hr during the first 30 hr, and at 4- to 5-hr intervals until 100 hr. Afterwards, and until the end of the experiment, they were taken at longer intervals. The overall operation of sampling the entire array of wells took less than 20 min, therefore each "snapshot" was considered to be representative of the indicated time.

During the second test continuous breakthrough curves of chloride and NOM were recorded at six sampling ports, specifically at wells 6, 13, 21, and 28 for depth 2.6 m, and wells 21 and 28 for depth 2.0 m. Samples were taken at 2 hr intervals for the first 3 days and the period after the tracer injection shut-down. Larger intervals were used during the remaining parts of the experiment. Continuous breakthrough curves were also recorded at the withdrawal wells in both tests.

Chloride concentrations were analyzed using standard wet chemical methods, and NOM was measured by a Total Carbon Analyzer Shimatzu model 5050 (Shimadzu Scientific Instruments, Columbia, MD).

Modeling Approach

The movement of the tracers was analyzed using a three-dimensional finite element flow and transport model (*3*). The governing equation describing the three-dimensional convective-dispersive transport of a reactive tracer in porous media is given by

$$\frac{\partial C}{\partial t}+\frac{\rho}{\theta}\frac{\partial S}{\partial x_i}\left(D_{ij}\frac{\partial C}{\partial x_j}\right)-v_i\frac{\partial C}{\partial x_i} \quad i,j=1,2,3 \qquad [1]$$

where C is the concentration of the dissolved tracer in units of mass per volume of liquid phase, S is the concentration of the tracer adsorbed on the aquifer matrix in units of mass of chemical per mass of soil, D_{ij} is the ijth component of the hydrodynamic dispersion tensor, v_i is the ith component of the velocity, ρ is the bulk density, and θ is the porosity.

Two types of reaction sites were considered: those that appeared to adsorb or to react rapidly with the chemical, inducing an instantaneous equilibrium, and those that adsorbed the solute more slowly, resulting in a kinetic reaction (*4*). Both processes were assumed to be independent. Total adsorbed concentration, S, was then given by the sum of the adsorbed concentration at each site, $S = S_1 + S_2$. Fraction S_1 accounted for the equilibrium model given by a linear isotherm, and fraction S_2 represented the time-dependent term, given by the first-order kinetic model

$$S_1 = K_3\frac{\theta}{\rho}C, \qquad [2]$$

$$\frac{\partial S_2}{\partial t} = K_1\frac{\theta}{\rho}C + K_2 \qquad [3]$$

where K_3 is a dimensionless partition coefficient, and K_1 and K_2 were the adsorption and desorption rate coefficients, in units of reciprocal time.

The aquifer encompassing a volume of 7 m × 9 m × 1.67 m was discretized into 10,868 finite elements for the numeric simulation. Conductivity values estimated from the slug tests were linearly interpolated using an inverse distance weight for the eight measurements nearest to the geometric center of each element. Detailed examination of the field data suggested that the interpolation scheme should have restricted the vertical search radius to one slug test interval to preserve the layered structure of the aquifer.

A porosity value of 0.25 was estimated to be appropriate for a fine sand material, and it was assumed to be constant through

the whole domain. Porosity changes were expected to be smaller than changes on the conductivity values and of less significance on the numerical solution. The longitudinal dispersivity was assumed to be 5 cm and the transverse dispersivity was set to 1.5 cm.

No-flow boundary conditions were defined at the top and bottom of the model, and constant head values were assigned to the lateral boundaries and to the nodes corresponding to the injection and withdrawal wells. These head values were estimated by analytically solving the Theis equation for the well doublet. For the nodes at the well locations, heads were modified until the correct flow was simulated by the numerical model. Estimated head values at the lateral boundaries were also corrected to account for the natural gradient of the site.

Initial concentrations equal to the aquifer background levels were assigned to all nodes, and a time dependent concentration boundary was defined for the nodes corresponding to the injection well to reflect the variation on the tracer input concentrations.

Results And Discussion

Hydraulic Conductivity Distribution

The results of the slug tests were analyzed following the methods by Hvorslev (*5*), Bouwer and Rice (*6*), and Cooper et al. (*7*). A detailed description of the slug test analysis will be presented elsewhere (Mas-Pla J, Yeh T-CJ, Williams TM, McCarthy JF. Hydraulic conductivity spatial variability at the Georgetown Site, South Carolina, submitted to Water Resources Research). Figure 2 shows the estimated hydraulic conductivity distribution with depth at a selected location, using the three different methods. In general, results of the three methods indicated a decrease of the hydraulic conductivity with depth. The hydraulic conductivity distribution along the cross-section in between the injection and the pumping wells (Figure 3) shows the layering of the aquifer and the important lateral variations of the hydraulic conductivity occurring within each layer. These variations in the upper layers may have been a result of root disturbances and other soil structures common in shallow coastal deposits.

It is worth noting, from Figures 2 and 3, that whereas the Hvorslev (*5*) and Bouwer and Rice (*6*) methods gave similar results, they differed notably from the Cooper et al. (*7*) values. Moreover, the variability of the conductivity values within layers was larger for the Cooper et al. method. Results of numerical simulations of the chloride plume of the first test (Table 1) by Yeh et al. (*8*) showed that the general migration of the chloride plume was reasonably replicated using conductivity data from either the Hvorslev (*5*) or the Cooper et al. (*7*) methods. For this reason, we only presented simulated results based on the hydraulic conductivity data set derived from the Hvorslev method.

Characteristics of the Chloride Plume Movement

Figure 4 shows the observed and the simulated chloride distributions (based on conductivity data sets estimated from both Hvorslev and Cooper et al. methods) corresponding to the May 1992 test along a cross-section between the injection and withdrawal wells. Two main features of the shape of the plume are worth notice: first, the movement of the chloride is responding to the layered structure of the hydraulic

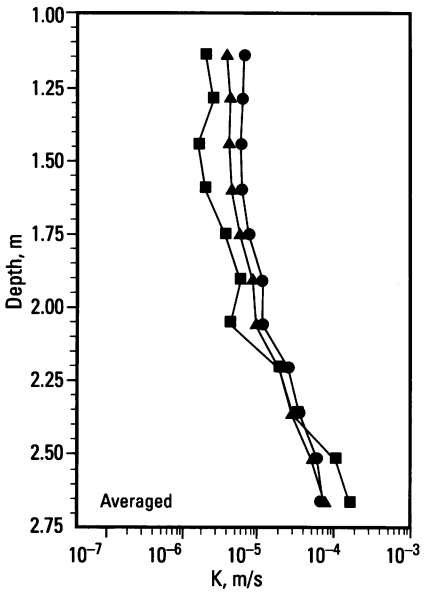

Figure 2. Hydraulic conductivity (in K) distribution with depth at a selected location.

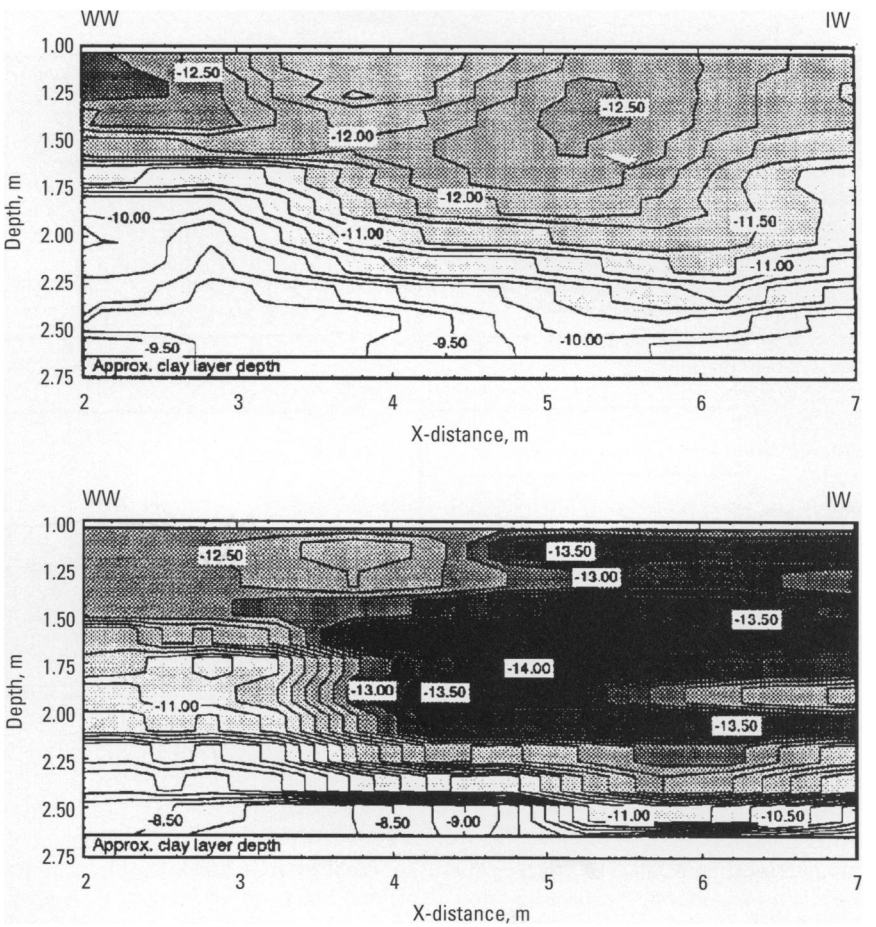

Figure 3. Hydraulic conductivity distributions in the cross-section in between the injection and pumping wells, estimated based on Hvorslev (top) and Cooper's (bottom) methods.

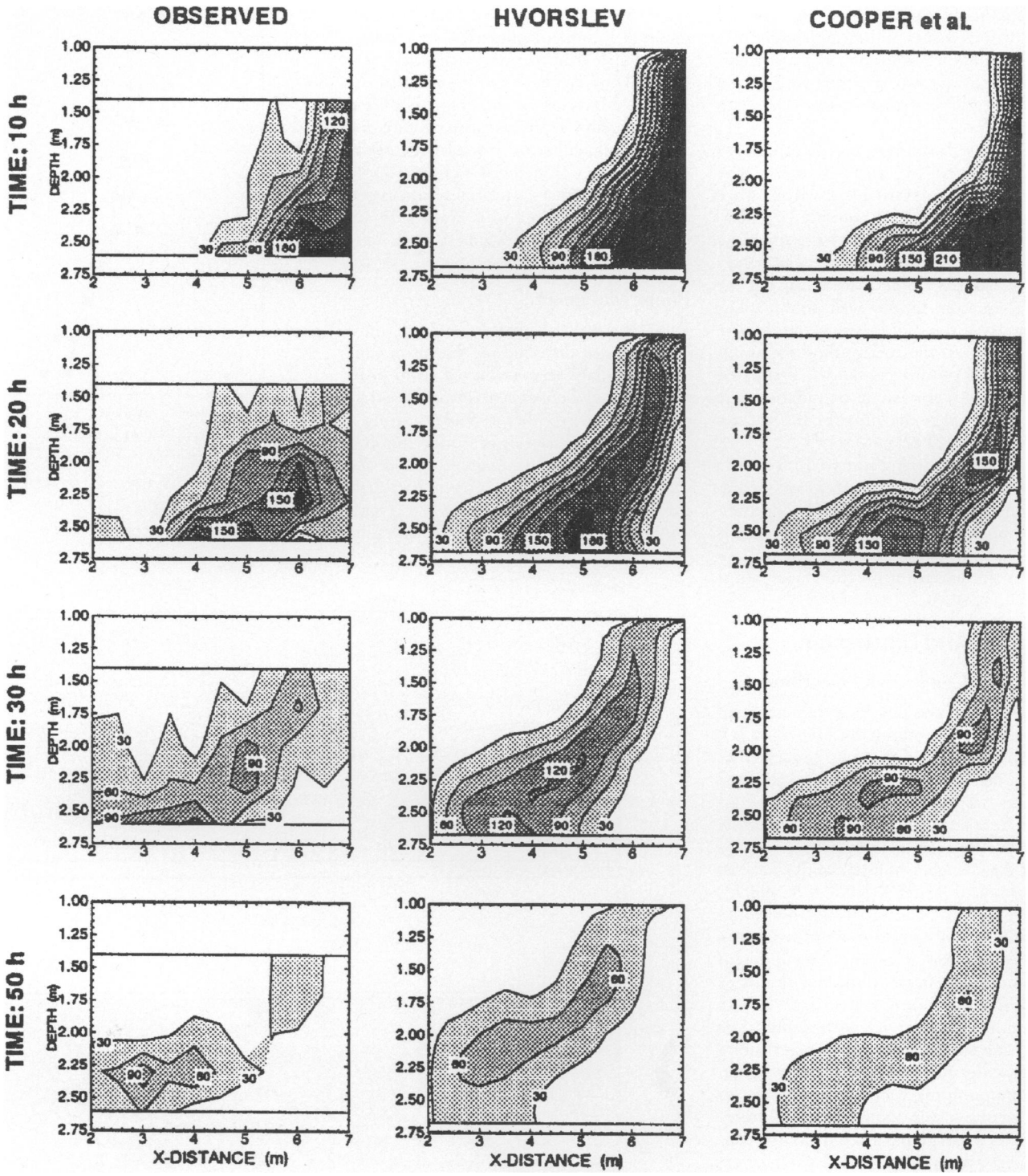

Figure 4. Observed and simulated chloride cross-sections for the May 1992 test.

conductivity (Figure 3). The effect of the stratification is manifested at early time when the plume has not reached the low permeability zone within the top layer (Figures 2,3). Second, at later times the low permeability zone had a significant impact on the migration of the tracer, creating a barrier that retarded the movement of the tracer at the upper part of the aquifer. This movement was satisfactorily simulated by the model, and it is fully attributed to the hydraulic conductivity distribution, and not to density effects.

Figure 5 depicts the observed and simulated breakthrough curves (using data

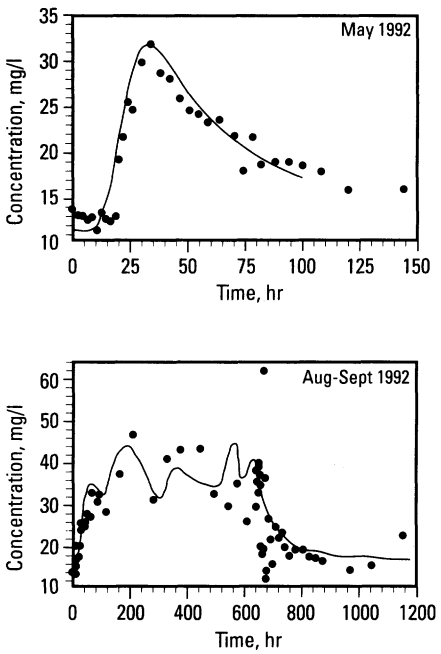

Figure 5. Observed (•) and simulated (—) breakthrough curves at the withdrawal well.

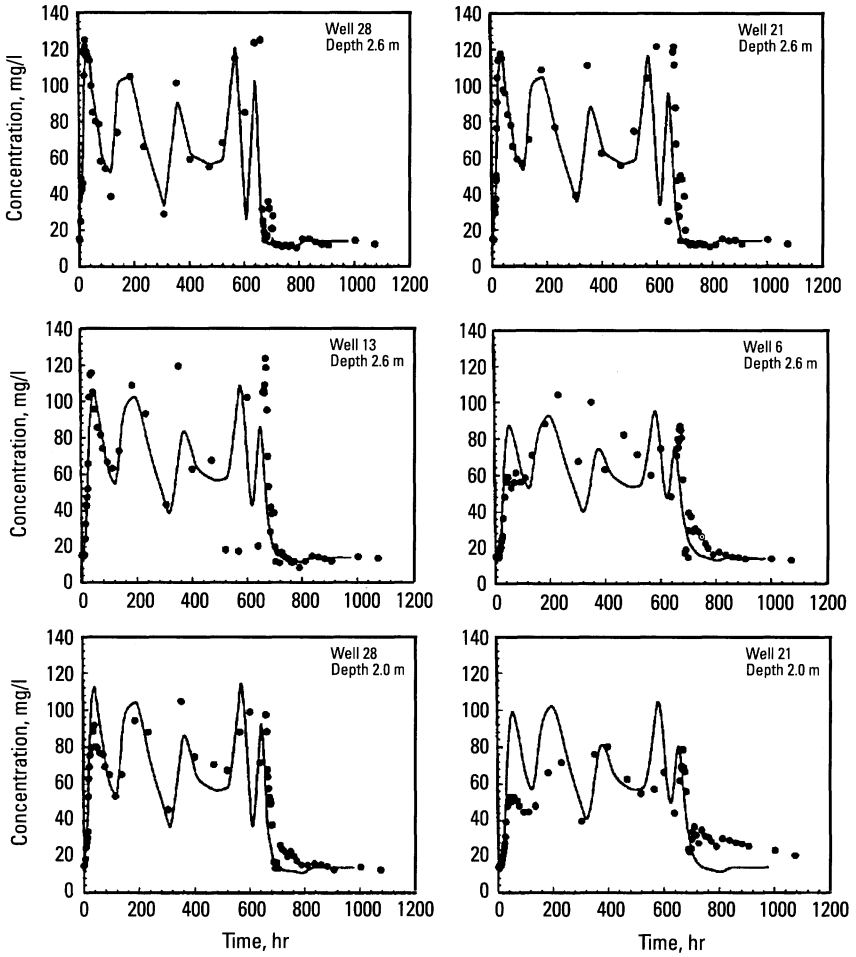

Figure 6. Observed (•) and simulated (—) chloride breakthrough curves at different wells.

based on Hvorslev's method) at the withdrawal well of both tests (i.e., May 1992 and August–September, 1992). It indicates that the integrated behavior of the plume can be well reproduced if a detailed knowledge of the hydrologic properties of the site is available. In addition, simulation results indicated that 75% of the extracted chloride mass came from the lower half of the aquifer during the first 1000 hours.

Point measurements were also satisfactorily simulated by the numerical model. For instance, the simulated breakthrough curves at several different wells shown in Figure 6 replicated the observed data with good accuracy, reproducing the individual peaks caused by the highly nonconstant input concentration.

NOM Plume Migration

The retardation factor of NOM versus chloride was estimated by the method of the moments (*9*); i.e, $R = \bar{t}_{NOM}/\bar{t}_{Cl}$ (Table 2). The first temporal moment, $\bar{t}$, describes the mean breakthrough of the solute, and it is not affected by nonequilibrium (kinetic) reactions (*10*). Because of the difference between the chloride and NOM input concentrations, chloride breakthrough curves were simulated using the NOM input sequence, and their first moment $\bar{t}_{Cl}^*$ was corrected using the ratio F, estimated from the "true" observed and simulated chloride data (Table 2). Retardation factors were found to range between 1.1 and 1.3, increasing with the travel distance. No retardation was observed for well 28 at depth 2.6 m.

A two-site sorption model (Equations 2, 3) with homogeneous and constant chemical parameters was used to reproduce NOM breakthrough curves. NOM arrival at locations close to the injection well (e.g., well 28) could be fairly well reproduced, at least for its ascending limb. As we move away from the injection well along the bottom layer, simulated concentrations systematically underestimate the observed ones. Failure to reproduce NOM breakthrough curves is illustrated at the withdrawal well (Figure 7). Furthermore, observed NOM breakthrough curves showed tailing, indicating a very slow desorption process.

Table 2. NOM retardation factors.

	$\bar{t}_{Cl}$ (obs)	$\bar{t}_{Cl}$ (sim)	F	$\bar{t}_{Cl}$ (NOM)	$\bar{t}_{Cl}^*$	$\bar{t}_{NOM}$	R
Depth 2.6 m							
Well 28	356.7	330.8	1.0783	338.5	365.0	347.8	0.95
Well 21	347.1	337.1	1.0297	345.1	355.3	372.9	1.05
Well 13	315.3	347.6	0.9077	356.6	323.6	417.6	1.29
Well 6	362.4	359.1	1.0092	370.5	373.9	482.6	1.29
Depth 2.0 m							
Well 28	360.2	338.8	1.0632	346.9	368.8	447.6	1.21
Well 21	386.4	357.0	1.0823	366.5	396.6	449.8	1.13
Pumping Well	463.5	422.1	1.0981	416.4	457.25	512.1	1.12

$\bar{t}_{Cl}$ (obs) and $\bar{t}_{Cl}$ (sim) are the first temporal moment of observed and simulated chloride plumes, respectively; $\bar{t}_{Cl}$ (NOM), first temporal moment of simulated chloride using NOM input concentration; $F = \bar{t}_{Cl}$ Obs/$\bar{t}_{Cl}$ Sim; $\bar{t}_{Cl}^* = \bar{t}_{Cl}$ (NOM) × F; $R = \bar{t}_{NOM}$ Obs/$\bar{t}_{Cl}^*$.

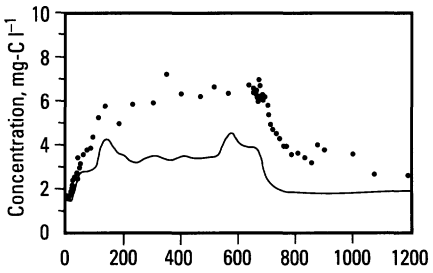

Figure 7. Observed (•) and simulated (—) NOM breakthrough curves at the withdrawal well.

The result of the simulation represented our first attempt to understand chemical processes controlling the transport of NOM in the field condition. Our simulation of the NOM breakthrough was not satisfactory. We postulate the reasons that caused the lack of fit in our simulation as follows:

Adequacy of the Model. Although the linear two-site sorption model has been reported to match NOM breakthrough data in laboratory experiments well (*2*), Jardine et al. reported that nonlinear models could improve NOM simulations. More recently, Gu (J Mas-Pla et al., unpublished data; B Gu et al., personal communication, 1993) showed that the desorption of NOM on iron oxide, using Georgetown water samples, was extremely slow. A nonlinear isotherm model and correct adsorption/desorption parameters may overcome the discrepancies between observed and simulated NOM data.

Movement of the NOM Fractions. Analysis of the NOM size fractions pointed out that the smallest size components (hydrophilic fraction) were transported almost conservatively, whereas the largest components (hydrophobic fraction) presented a larger retardation. Therefore, different NOM components present distinct sorptive properties, which could not be integrated in a single conceptual model to describe the bulk NOM movement. Different site competition rates along the flow path may also occur.

Spatial Variability of the Sorption Rates. Inconsistent differences between observed and simulated NOM breakthrough curves at different locations suggested that sorption rates may vary significantly throughout the domain. Different matrix composition as well as different adsorbed concentrations at the initial moments may cause such variability. Underestimation of the breakthrough curves using a constant parameter model indicates that adsorption may indeed decrease with distance (this would be expected if hydrophobic fractions of NOM are removed along the flow plane). In fact, identical retardation factors were estimated at wells 13 and 6 (Table 2).

A detailed three-dimensional characterization of the hydraulic conductivity field was necessary to successfully reproduce the movement of a conservative tracer (chloride). Significant conductivity variations in the sandy aquifer retarded the tracer movement in the upper layers of the aquifer and forced the tracer to move almost exclusively through the bottom layer, illustrating the importance of the hydrologic heterogeneity.

Results of our preliminary analysis of NOM data suggest that a simple adsorption–desorption model may not adequately describe the transport of NOM at a field scale, nor its interactions with the aquifer matrix. Different mechanisms for adsorption and desorption processes appear to be responsible for our failure to reproduce the observed NOM breakthrough. Further, the distinct chemical properties of each NOM fraction and the spatial variability of the sorption reactions may affect the NOM migration, and they should be considered in future studies.

REFERENCES

1. McCarthy JF, Zachara JM. Subsurface transport of contaminants. Environ Sci Technol 23(5):496–502 (1989).
2. Jardine PM, Dunnivant FM, Selim HM, McCarthy JF. Comparison of models for describing the transport of dissolved organic carbon in aquifer columns. Soil Sci Soc Am J 56:393–401 (1992).
3. Srivastava R, Yeh T-CJ. A three-dimensional numerical model for water flow and transport of chemically reactive solute through porous media under variably saturated conditions. Adv Water Resour 15:275–287 (1992).
4. Cameron DA, Klute A. Convective-dispersive solute transport with a combined equilibrium and kinetic adsorption model. Water Resour Res 13:183–188 (1977).
5. Hvorslev MJ. Time Lag and Soil Permeability in Groundwater Observations. US Army Corps of Engineers, Waterways Exp. Station Bull, 36, Vicksburg, MS, 50 (1951).
6. Bouwer H, Rice RC. A slug test for determining hydraulic conductivity of unconfined aquifers with complete or partially penetrating wells. Water Resour Res,12(3):423–428 (1976).
7. Cooper HH Jr, Bredehoeft JD, Papadopulos IS. Response of a finite diameter well to an instantaneous charge of water. Water Resour Res 3(1):263–269 (1967).
8. Yeh T-CJ, Mas-Pla J, Williams TM, McCarthy JF. Three-dimensional simulation of a chloride plume in a coastal sandy aquifer, Georgetown site, SC. American Geophysical Union Fall Meeting, San Francisco, December 7–11, 1992, EOS Transactions 73(43):171 (1992).
9. Roberts PV, Goltz MN, Mackay DM. A natural gradient experiment on solute transport in a sand aquifer, 3. Retardation and mass balances for organic solutes. Water Resour Res 22:423–428 (1976).
10. Brusseau ML, Rao PSC. Sorption nonideality during organic contaminant transport in porous media. CRC Crit Rev Environ Control 19(1):33–99 (1989).